ThinK: Thinner Key Cache by Query-Driven Pruning

Yuhui Xu^{1*} Zhanming Jie¹ Hanze Dong¹ Lei Wang¹

Xudong Lu² Aojun Zhou² Amrita Saha¹ Caiming Xiong¹ Doyen Sahoo¹

¹Salesforce AI Research ² The Chinese University of Hong Kong

Abstract

Large Language Models (LLMs) have revolutionized the field of natural language processing, achieving unprecedented performance across a variety of applications by leveraging increased model sizes and sequence lengths. However, the associated rise in computational and memory costs poses significant challenges, particularly in managing long sequences due to the quadratic complexity of the transformer attention mechanism. This paper focuses on the long-context scenario, addressing the inefficiencies in KV cache memory consumption during inference. Unlike existing approaches that optimize the memory based on the sequence lengths, we uncover that the channel dimension of the KV cache exhibits significant redundancy, characterized by unbalanced magnitude distribution and low-rank structure in attention weights. Based on these observations, we propose ThinK, a novel query-dependent KV cache pruning method designed to minimize attention weight loss while selectively pruning the least significant channels. Our approach not only maintains or enhances model accuracy but also achieves a reduction in memory costs by over 20% compared with vanilla KV cache eviction methods. Extensive evaluations on the LLaMA3 and Mistral models across various long-sequence datasets confirm the efficacy of ThinK, setting a new precedent for efficient LLM deployment without compromising performance. We also outline the potential of extending our method to value cache pruning, demonstrating ThinK's versatility and broad applicability in reducing both memory and computational overheads.

^{*}Email: {yuhui.xu, ajie, hanze.dong, leiwang, amrita.saha, cxiong, dsahoo}@salesforce.com

Contents

T	Intr	oduction	3
2	Obs	servations	4
3	Thi	nK	5
	3.1	Preliminary Study of KV Cache Optimization	6
	3.2	Query-Driven Pruning	7
	3.3	Implementations	8
4	Exp	periment Results	8
	4.1	Settings	8
	4.2	Results on LongBench	9
	4.3	Results on Needle-in-a-Haystack	10
	4.4	Ablation Studies	11
5	Rela	ated Work	15
6	End	Note and Future Direction	15
A	Add	litional Experimental Details	20
	A.1	Value Cache Pruning	20

1 Introduction

Large language models (LLMs) (Hadi et al., 2023; Brown et al., 2020; OpenAI, 2023; Touvron et al., 2023a,b; Scao et al., 2022; Reid et al., 2024) have emerged as a dominant paradigm in natural language processing, achieving state-of-the-art performance across various tasks. A key principle, the Scaling Law (Kaplan et al., 2020), suggests that LLMs exhibit emergent abilities as model size increases, enhancing their capacity to understand context and handle long sequences (Xiong et al., 2023). This capacity growth allows LLMs to generate coherent and contextually accurate responses and enables various downstream applications, such as document summarization (Zhang et al., 2019, 2024a), code generation (Chen et al., 2021b), and conversational AI (Bordes et al., 2016; OpenAI, 2022), .

Despite their success in various applications, the generation of LLMs incurs significant expenses, which escalate with increasing model size and sequence length. Notably, both the training (Strubell et al., 2020; Hoffmann et al., 2022; Dong et al., 2024a) and inference (Ainslie et al., 2023) stages involve frequent generation by LLMs, further contributing to these costs. Consequently, efficient LLMs have gained popularity in recent years (Hu et al., 2021; Wan et al., 2023). To address these challenges, quantization (Frantar et al., 2022; Lin et al., 2024; Dettmers et al., 2024; Xu et al., 2023) and pruning methods (Frankle and Carbin, 2018; Blalock et al., 2020) are employed to reduce model size. Additionally, managing long sequences presents another cost due to the transformer attention mechanism. The quadratic complexity of the attention mechanism results in substantial computational burden when dealing with long sequences, scaling poorly with sequence length. Therefore, effective management of long sequences is essential for the practical deployment of LLMs. In this paper, we focus on the long-context scenario and aim to reduce the memory consumption associated with lengthy sequences.

Specifically, the number of KV cache parameters is the product of batch size B, sequence length S, number of layers L, number of heads N, channel size of each head D, i.e., $\mathbf{K}, \mathbf{V} \in \mathbb{R}^{B \times S \times L \times N \times D}$, which need to be stored in the GPU memory during inference. To reduce memory and computational costs during inference, efficiency can only be achieved by pruning the dimensions across S, L, N, D or performing quantization over the caches. It is well-acknowledged that token importance tends to be sparse. Consequently, KV eviction algorithms have been proposed to minimize the KV cache memory cost from dimension S (Xiao et al., 2023b; Li et al., 2024; Zhang et al., 2024c; Leviathan et al., 2023). Additionally, inter-layer redundancy has been explored (Liu et al., 2024a; Wu and Tu, 2024; Brandon et al., 2024) to address the layer dimension L. Despite these advances, existing methods have largely overlooked the channel dimension D. In this paper, we highlight that the magnitude across Key cache channel dimensions is significantly unbalanced. Additionally, we observe that the attention weights exhibit a low-rank structure. Based on these findings, we hypothesize that the channel dimension of the key cache exhibits redundancy. Consequently, we explore the redundancy of KV cache tensors specifically from dimension D, aiming to devise effective strategies that reduce costs without compromising performance.

In our paper, we propose a simple yet effective method – **ThinK**, for KV cache pruning. To pinpoint the least significant channels, we formulate the task as an optimization problem, aiming to minimize the loss in attention weights attributable to pruning. To effectively address this problem, we establish a novel query-dependent criterion that assesses the importance of each channel. Using this criterion, we then select the most critical channels in a greedy fashion. We evaluate **ThinK** using the LLaMA3 (Meta, 2024) and Mistral (Jiang et al., 2023) models and validate its effectiveness across various long-sequence datasets. The results indicate that when paired with token eviction methods, ThinK not only achieves comparable or superior accuracy but also reduces KV cache memory costs by more than 20%.

Contributions. This work pioneers the investigation into the sparsity structure of the channels in the KV cache. Specifically, we discovered that the activated key cache is sparse given a specific query. This insight allows us to prune the key cache channels using a query-induced norm. Inspired by this phenomenon, we

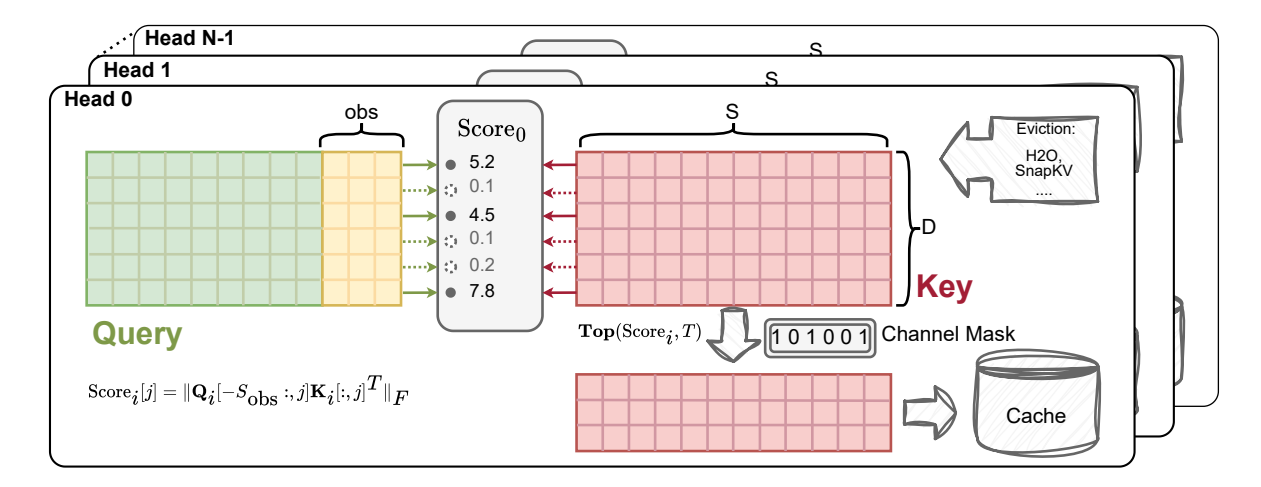


Figure 1: An illustration of the pruning procedure of ThinK. Within each head, scores are calculated for each channel, and only the top T channels out of D are selected for retention. A binary channel mask, along with the pruned keys, is subsequently stored in the cache memory.

introduce a plug-and-play method ThinK, the first channel pruning method specifically designed for KV cache. ThinK reduces the dimensionality of the cache channel, leading to linear savings in both memory and computational requirements. As plug-and-play techniques, our proposed ThinK is orthogonal to other KV cache compression schemes (e.g. KV cache eviction, quantization). Our extensive experiments demonstrate the remarkable efficiency of ThinK on LLaMA-3 and Mistral models. Furthermore, we explore the promising potential of extending ThinK to value cache pruning (ThinKV) in specific scenarios, highlighting the broad applicability of our method.

2 Observations

We identify several key observations that motivate our approach to prune the channel of KV-Cache. Specifically, we visualize the magnitude of KV-cache and perform singular value decomposition of the attention in LLaMA3-8B model. We show the visualization for certain heads and layers for illustration purposes.

Magnitude of KV-Cache Channel Figure 2 visualizes the absolute values of key and value cache across the tokens in each channel¹. Consistent with previous findings (Lin et al., 2024; Xiao et al., 2023a; Liu et al., 2024b), we observe that only certain channels have significant magnitudes in the key cache, whereas the value cache lacks obvious patterns. For instance, the absolute value around 50th channel of key cache has much larger magnitudes than other channels for all tokens in layer 14 (Figure 2 (a)). The same observation applies to 50th and 150th channels of the first head in layer 20 (Figure 2 (c)). Given such an observation, Liu et al. (2024b) proposed to perform quantization over the channels of the key cache based on such observations. In addition to channel quantization, the observation also suggests that it is feasible to prune away certain key cache channels that contribute less to the attention mechanism. Moreover, channel quantization and pruning techniques are orthogonal such that they can be utilized concurrently to enhance model efficiency.

 $^{^{1}} We use the visualization code from \verb|https://github.com/jy-yuan/KIVI/tree/main/vis.|$

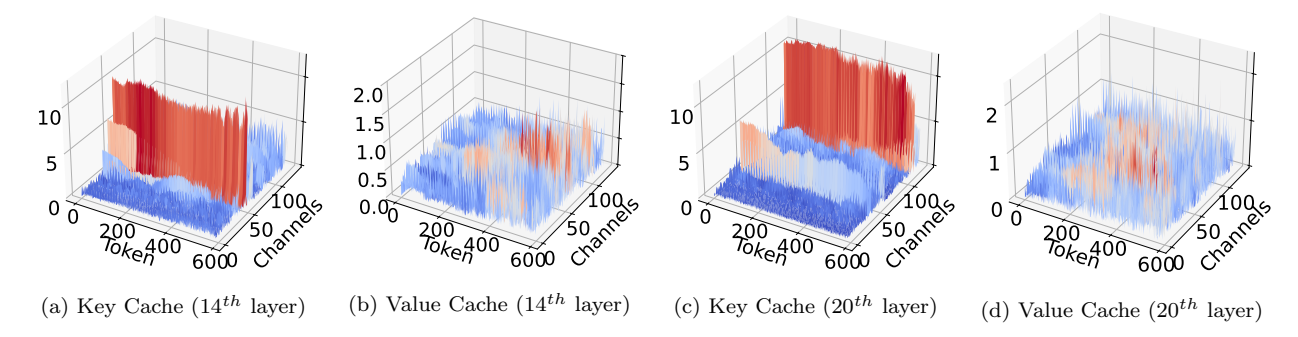


Figure 2: Magnitude of key and value cache for LLaMA3-8B. The first head of layer 14 and layer 20 of LLaMA3-8B is selected to visualize the magnitude of the key and value caches. We observe that the magnitudes of the key cache channels vary differently, whereas the channels of the value cache do not exhibit such variation.

Singular Value Analysis We conducted singular value decomposition (SVD) (Demmel, 1997) on the attention of the specified layers to investigate their principal components. The singular values derived from SVD capture the effective rank of the attention matrix, indicating how the information is distributed across different components.

$$\mathbf{U}, \mathbf{\Sigma}, \mathbf{V} = \text{SVD}\left(\text{softmax}\left(\frac{\mathbf{Q}\mathbf{K}^T}{\sqrt{D}}\right)\right), \quad \text{Energy}_i = \frac{\sigma_i^2}{\sum_i \sigma_i^2}$$
 (1)

Figure 3 (a) illustrates the energy distribution of the singular values, plotted in log scale to enhance the visibility of differences among them. Notably, only a few singular values exhibit high energy levels exceeding 0.01 across all heads and layers, highlighting their relative significance. This observation aligns with previous findings (Bhojanapalli et al., 2021), where a small subset of singular values often captures most of the information in attention mechanisms. In addition, the rapid decay of the energy suggests that a low-rank approximation can effectively capture the essential information in the key cache.

Figure 3 (b), the normalized cumulative energy sum reveals that the top 50 singular values account for over 90% of the total energy. These findings suggest that the attention matrix is inherently low-rank (Wang et al., 2020; Chen et al., 2021a; Dong et al., 2024b), indicating that the key cache can be approximated using low-dimensional vectors (Singhania et al., 2024).

3 ThinK

Notations. We use uppercase letters (e.g., X, Y) to denote scalar values and boldface uppercase letters $(e.g., \mathbf{Q}, \mathbf{K})$ to denote matrices and tensors. The notation $\|\cdot\|_p$ denotes the l_p -norm for vectors. Unless otherwise specified, $\|\cdot\|$ denotes the l_2 -norm. The Frobenius norm is denoted by $\|\cdot\|_F$. The floor function is denoted by $\|\cdot\|_F$, and the ceiling function is denoted by $\|\cdot\|_F$.

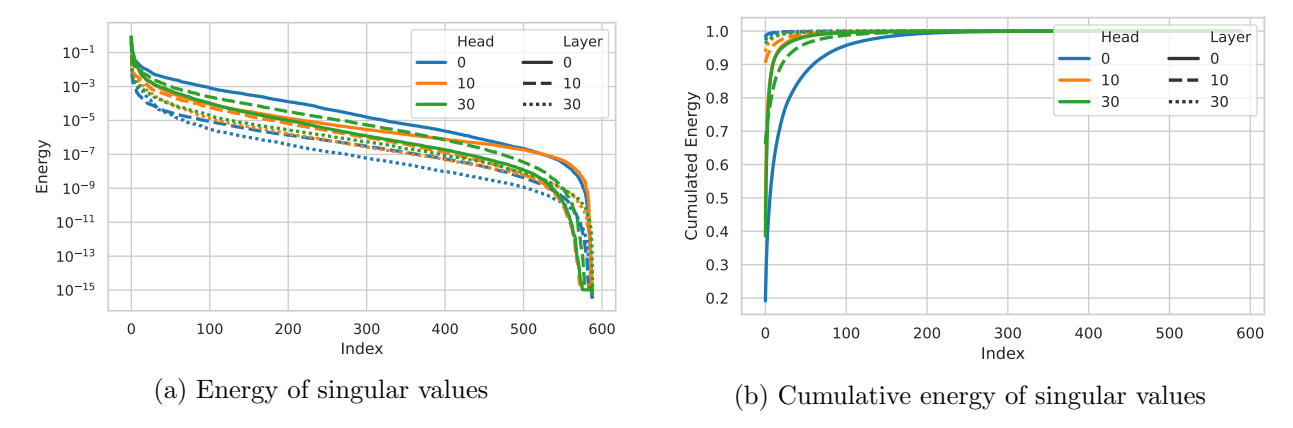


Figure 3: The energy and cumulative energy of the singular values.

3.1 Preliminary Study of KV Cache Optimization

In scenarios with extended contexts or batch processing, the main limitations in terms of memory and speed are due to the handling of the KV cache size. Considering a batch of requests to a Large Language Model (LLM) service that provides a long input prompt consisting of tokens $[x_{B1}, ..., x_{BS}]$, the total KV cache size can be computed as follows:

$$2 \times B \times S \times L \times N \times D,\tag{2}$$

where L is the number of layers, N is the number of heads, D is the head dimension. The KV cach size grows linearly as the batch size B and sequence length S. For a model with multihead attention (MHA) (Vaswani et al., 2017), such as LLaMA2-7B (Touvron et al., 2023b), a context length of 2048 and a batch size of 13 require storing a 13 GB KV cache, which is equivalent to the size of the model parameters. The KV cache must be transferred from off-chip memory (HBM) (Jia et al., 2018) to on-chip memory (cache) for each token generated, leading to a memory bottleneck. This substantial memory demand highlights the challenges in managing large-scale models and the need for efficient memory utilization strategies. Current methods optimize the KV cache based on the sequence length S (Xiao et al., 2023b; Zhang et al., 2024c; Li et al., 2024) and precision (Hooper et al., 2024; Liu et al., 2024b). We will introduce a new method, **ThinK**, to optimize it from the perspective of the number of head dimensions D.

Table 1: Performance comparison of pruning K cache by l_p norm on LongBench.

		Single	-Docum	Document QA		Multi-Document QA			Summarization				earning	Synt	hetic	C		
Method	dλ	NrtvQA	Oasper	MF-en	HotpotQA	2WikiMQA	Musique	GovReport	QMSum	MultiNews	TREC	TriviaQA	SAMSun	PCount	P^{Re}	rcc	RB-P	Avg.
H2O	0	23.52	17.93	34.68	42.11	33.52	19.92	22.11	22.56	23.82	41.00	90.46	40.20	5.87	69.50	56.71	51.69	37.23
$+l_1$	30	23.38	17.15	34.99	40.56	31.49	19.90	21.37	22.13	23.44	40.50	90.10	40.65	5.41	69.00	58.64	54.99	37.11
$+l_1$	40	23.51	15.40	34.37	40.71	31.28	20.24	21.25	22.29	22.54	38.50	89.22	39.27	5.87	68.33	58.47	54.33	36.60
$+l_2$	30	23.98	17.04	35.19	39.27	31.29	20.4	21.62	22.46	23.34	40.5	89.75	40.71	5.54	68.67	60.12	58.52	37.40
$+l_2$	40	23.76	16.23	32.19	40.23	32.13	20.69	21.3	22.25	23.2	39.5	89.61	40.24	5.66	69.0	60.09	59.45	37.22
SnapK	V 0	24.84	23.96	38.77	42.75	34.55	20.87	22.26	22.61	23.97	70.00	90.52	40.29	5.81	69.50	59.04	51.81	40.10
$+l_1$	30	24.43	24.63	40.11	41.83	33.47	21.22	21.47	22.41	23.73	66.50	90.39	40.20	5.70	68.10	61.04	55.37	40.04
$+l_1$	40	24.58	24.87	39.30	42.76	31.95	20.47	20.95	22.22	23.42	55.50	90.22	39.13	5.82	68.39	60.71	56.10	39.15
$+l_2$	30	24.47	24.73	38.16	41.86	32.23	20.23	21.59	22.45	23.77	67.5	90.33	40.31	5.7	68.42	62.65	60.07	40.28
$+l_2$	40	24.52	23.75	38.35	42.42	32.96	20.39	21.21	22.28	23.41	60.00	90.20	39.59	5.75	68.29	61.96	60.59	39.74

Magnitude base Pruning: Based on the observations in Figure 2 which depicts the significant variation in the magnitudes across different channels, one straightforward criterion is to use the norm of the magnitude

to measure the importance of different channels in key cache.

$$M_{n,d} = \|K[n,:,d]\|_{p}.$$
(3)

Given pruning ratio λ , We only keep $T = \lfloor (1 - \lambda)D \rfloor$ most important channels among the D channels of each head:

$$I = \mathbf{Top}_T(M, T) \tag{4}$$

where $\|\cdot\|_p$ is the l_p norm of each channel. $n \in [1, N]$ and $d \in [1, D]$ are indicators of heads and channels in key cache. $I \in (\mathbb{Z}^+)^{N \times T}$ stores the indicators of the top T values in tensor M per head.

In Table 1, we present the results of key cache pruning with various pruning ratios applied to the LLaMA3-8B model. We utilize the l_1 and l_2 norms as criteria for evaluation, and validate performance using the LongBench benchmark (Bai et al., 2023). Compared to the baseline methods, H2O (Zhang et al., 2024c) and SnapKV (Li et al., 2024), both with a KV length of 512, we further prune the channels of the key cache. A 30% pruning ratio can maintain accuracy; however, increasing it to 40% results in significant performance degradation, especially for l_1 norm based pruning. The results of magnitude-based pruning support our assumption that the key cache is redundant in the channel dimension. These results also indicate the need for a better pruning matrix to achieve higher pruning ratios effectively.

3.2 Query-Driven Pruning

For each head, the attention scores are computed using the queries and keys, and then applied to the values. The formula for the attention for head i is:

$$Attention(\mathbf{Q}_i, \mathbf{K}_i, \mathbf{V}_i) = \operatorname{softmax}(\frac{\mathbf{Q}_i \mathbf{K}_i^T}{\sqrt{D}}) \mathbf{V}_i$$
 (5)

where $\mathbf{Q}_i, \mathbf{K}_i, \mathbf{V}_i \in \mathbb{R}^{S \times D}$. When pruning one channels of \mathbf{K}_i , the corresponding channels in \mathbf{Q}_i will also be removed. We aim to find the optimal subset of channels to prune, denoted by the selection matrix $\mathbf{S} \in \{0,1\}^{D \times D}$, where \mathbf{S} is a diagonal matrix with binary entries (1 for keeping a channel, 0 for pruning it). To better maintain the performance after pruning the channels, we minimize the Frobenius norm of the difference between the original and pruned attention weights:

$$\min_{\mathbf{S}} \|\mathbf{Q}_i \mathbf{K}_i^T - \mathbf{Q}_i \mathbf{S} (\mathbf{K}_i \mathbf{S})^T \|_F$$
 (6)

Given a pruning ratio λ , it can further expanded as:

$$\min_{\mathbf{S}} \quad \|\mathbf{Q}_{i}\mathbf{K}_{i}^{T} - \mathbf{Q}_{i}\mathbf{S}\mathbf{K}_{i}^{T}\|_{F}$$
subject to $\operatorname{trace}(\mathbf{S}) = \lfloor (1 - \lambda)D \rfloor$

$$\mathbf{S} = \operatorname{diag}(s_{1}, s_{2}, \dots, s_{D}), \text{ where } s_{i} \in \{0, 1\}$$
(7)

For simplicity, we use greedy algorithm to optimize S. To achieve the pruning goal, we define a criterion for evaluating the importance of each channel and greedily select the channels with largest scores:

$$Score_{i}[j] = \|\mathbf{Q}_{i}[:,j]\mathbf{K}_{i}[:,j]^{T}\|_{F}$$
(8)

$$I_i = \mathbf{Top}_T(\mathrm{Score}_i, T)$$
 (9)

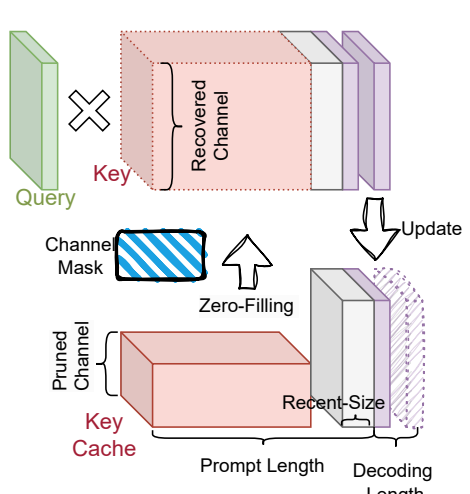
Here's a detailed explanation of why it optimizes the selection matrix. The score_i[j] measures the magnitude of the interaction between the query and key vectors for channel j in each head i. By selecting channels

with the highest interaction magnitudes, we aim to retain the most significant contributions to the attention mechanism. This criterion ensures that the selected channels preserve the primary information flow in the attention computation, thereby minimizing the loss of important information.

Observation Window. Based on the observations in SnapKV (Li et al., 2024) that the last window of input sequence recognizes highly similar attention allocation pattern with the actual generation. To reduce the computation cost, we only use the last S_{obs} window to calculate the score: $\|\mathbf{Q}_i[-S_{obs}:,j]\mathbf{K}_i[:,j]^T\|_F$.

3.3 Implementations

Following SnapKV, we focus on the long context input scenario. We opt not to prune the most recent tokens and newly generated keys. Consequently, our key-value (KV) cache will store two distinct categories of keys: one subset consists of pruned keys with a reduced channel size, while the other retains keys at their original size. Additionally, we maintain a binary mask to indicate which channels have been pruned. Note that the memory overhead associated with this mask is negligible. Figure 4 illustrates one implementation of our method during the decoding stage. The pruned keys are first zero-filled using the mask to restore them to their original size, and then concatenated with the unpruned keys. This implementation can be effectively integrated with optimization techniques such as FlashAttention (Dao, 2023). The second implementation involves initially pruning the Query using the mask. The pruned Query is then multiplied by the pruned Key, while the unpruned Query is applied to the unpruned Key. Subsequently,



pruned Query is applied to the unpruned Key. Subsequently, Figure 4: Implementation during decoding. the two outputs are concatenated. In theory, this implementation has lower computational costs.

4 Experiment Results

In this section, we conduct extensive experiments to evaluate the effectiveness of **ThinK** on performance and memory reduction. First, we introduce benchmark datasets, baseline methods, and implementation details in Section 4.1. Next, we report the performance of our KV pruning method with two different KV compression methods in long-context scenarios in Section 4.2. Finally, we present the results of ablation experiments in Section 4.4.

4.1 Settings

Benchmark Datasets. We perform evaluations of our method with state-of-the-art KV cache compression methods on two widely used benchmarks: LongBench and Needle-in-a-Haystack. LongBench (Bai et al., 2023) is designed to comprehensively evaluate LLM's long context understanding capabilities. It includes 17 datasets covering six different tasks: single-document QA, multi-document QA, summarization, few-shot learning, synthetic tasks, and code completion. The average input length of LongBench is 6,711 words, which necessitates reducing the KV cache to lower memory usage for inference. Needle-in-a-Haystack (Kamradt, 2023) is a recent popular test challenge that requires models to accurately identify a small piece of information ("needle") in a long document ("haystack"), where the needle is placed at a random position. This challenge can test if KV cache compression methods still retain the small piece of critical information.

Table 2: Performance comparison of Key cache pruning on LLaMA3-8B by ThinK on LongBench.

	Single	-Docum	•		i-Documen	•		mmariza			-shot Le	earning	Synt	hetic	Code		
Method	NrtvQA	Qasper	MF-en	HotpotQA	2WikiMQA	Musique	GovRepor	t QMSum	MultiNews	TREC	TriviaQ.A	SAMSum	PCount	PRe	Lcc	RB-P	Avg.
A T T 7737	05.50	00.05					KV-s	ize Full						00.05	FO 00	F 4 0 F	41.00
ALL KV	25.56	32.27	39.71	43.56	35.09	21.18	28.71	23.26	26.64	73.50	90.48	42.33	4.80	69.25	59.29	54.05	41.86
								ize 128									
H2O	22.12	13.20	31.61	37.79	32.71	18.45	20.32	22.02	21.10	38.50	87.75	39.14	5.83			50.97	
+ThinK(40)		14.55	29.49	38.63	30.84	18.90	20.12	21.96	20.68	38.50	86.38	38.40	5.50			56.12	
+ThinK(50		14.06	28.67	_ 38.35 _	30.21	_ 17.87	19.69	_ 21.94	19.95	38.50	87.14	38.07	4.92			56.66	35.44
SnapKV		13.55	32.64	38.75	29.64	18.73	18.98	21.62	20.26	45.00	88.36	37.64	5.13			51.82	
+ThinK(40		14.67	32.49	36.25	28.63	18.80	18.93	21.49	20.14	44.50	88.11	38.32	5.75			55.89	
+ ThinK (50)) 21.79	14.73	32.03	37.52	27.86	18.28	18.50	21.52	19.71	43.50	86.00	38.35	5.59	69.50	57.96	56.96	35.61
							KV-s	ize 512									
H2O	23.52	17.93	34.68	42.11	33.52	19.92	22.11	22.56	23.82	41.00	90.46	40.20	5.87	69.50	56.71	51.69	37.23
+ThinK(40)		17.80	33.80	40.39	30.70	19.09	21.82	22.51	23.78	41.00	90.16	40.67	5.15			57.58	
+ThinK(50)		16.96	35.76	39.47	30.29	18.67	21.39	22.59	23.06	41.00	89.81	40.35	5.23	69.33	60.20	58.34	37.29
+ThinK(60)		14.83	32.62	38.47	30.97	19.81	20.80	22.04	21.60	40.00	88.79	38.90	5.36			57.65	
SnapKV	24.84	23.96	38.77	-42.75	34.55	20.87	22.26	22.61	23.97	70.00	90.52	40.29	5.81			51.81	
+ThinK(40)		25.44	37.03	41.87	33.45	20.58	21.77	22.42	24.16	70.00	90.39	40.29	6.06				40.55
+ThinK(50)		25.10	37.06	41.58	32.34	20.60	21.61	22.44	23.66	69.50	90.39	39.70	5.84			59.42	40.34
+ ThinK (60)) 25.98	22.77	38.37	40.44	33.19	19.90	20.84	22.21	22.55	59.00	90.32	38.12	6.39	69.50	59.14	58.40	39.20
							KV-si	ze 1024									
H2O	25.62	22.16	36.81	41.01	33.53	19.41	23.28	22.65	25.41	46.50	90.82	41.78	5.79	69.25	59.69	55.50	38.70
+ThinK(40)) 25.52	21.93	37.17	41.56	31.22	20.17	22.89	22.95	25.21	47.00	90.74	41.34	5.57	69.50	62.58	58.67	$\overline{39.00}$
+ThinK(50)	25.41	22.19	37.64	40.92	31.27	18.66	22.17	22.22	24.84	46.50	90.34	40.59	5.20	69.50	61.71	57.99	38.57
+ThinK(60)	24.06	17.80	37.85	38.63	29.98	19.40	21.41	22.32	23.42	44.50	90.16	39.43	5.84	69.50	58.31	58.73	37.58
$\overline{\mathrm{Snap}}\overline{\mathrm{K}}\overline{\mathrm{V}}$	24.62	$^{-}2\overline{5}.99$	37.64	43.84	34.99	20.00	$\overline{24.28}$	22.39	25.63	$^{-}$ $7\overline{2}.\overline{5}$	-90.56	$-40.\overline{4}1$	5.36				40.88
+ThinK(40)		27.72	38.60	43.16	32.44	20.67	24.21	22.79	25.56	71.50	90.45	40.94	5.93	69.50	62.77	59.45	41.29
+ThinK(50)) 24.82	27.26	39.66	42.82	32.09	19.56	23.52	22.48	25.34	71.50	90.43	40.74	5.20			59.75	41.07
+ThinK(60)	24.46	27.35	38.22	41.96	31.64	20.18	21.89	22.83	23.68	70.00	90.19	38.69	6.10	69.50	58.87	59.26	40.30
							KV-si	ze 2048									
H2O	25.56	26.85	39.54	44.30	32.92	21.09	24.68	23.01	26.16	53.00	90.65	41.84	4.91	69.25	58.43	51.31	39.59
+ThinK(40		26.31	39.20	42.96	31.81	20.53	24.23	23.35	25.90	53.50	90.56	41.03	5.52			59.00	
+ThinK(50)		25.37	38.82	42.32	31.27	20.50	23.78	23.21	26.03	53.00	90.37	40.86	5.13			58.95	39.75
+ThinK(60)		22.14	37.77	40.13	29.50	20.26	22.09	22.76	24.78	49.50	90.16	39.69	5.56			58.78	
$\overline{Snap}K\nabla \stackrel{\sim}{-}$	$25.8\overline{6}$	$^{-}2\overline{9}.5\overline{5}$	41.10	- _{44.99} -	35.80	- <u>2</u> 1.81	$\overline{25.98}$	- 2 3.40	-26.46	$7\overline{3.50}$	- 90. 5 6-	$-41.\overline{6}6^{-}$	5.17	$\overline{69.25}$	58.67	51.52	41.58
+ThinK(40)) 25.41	29.79	39.21	43.35	33.96	21.49	25.78	23.11	26.23	73.00	90.56	41.79	5.81	69.50	62.45	59.19	41.91
+ThinK(50)	25.00	30.25	39.27	43.23	32.93	21.24	25.16	23.01	26.5	73.00	90.37	41.26	5.45	69.50	62.3	59.84	41.77
+ThinK(60)	24.89	28.88	40.44	41.30	29.99	21.34	23.48	22.9	24.99	72.50	90.36	38.5	5.71	69.50	59.77	59.50	40.88

Baseline Approaches. The baseline methods include Heavy Hitter Oracle (H2O) and SnapKV, both of which are the state-of-the-art KV cache compression methods but use different strategies for selecting KV cache. H2O (Zhang et al., 2024c) is designed to reduce memory usage by dynamically balancing recent tokens and Heavy Hitter (H2) tokens, where H2 tokens are a small set of tokens that contribute most of the value when computing attention scores. SnapKV (Li et al., 2024) automatically compresses KV caches by selecting clustered important KV positions for each attention head. This is inspired by the fact that each attention head has a specific pattern, focusing on certain attention features during generation.

Implementation Details. In this paper, we use LLaMA3-8B-Instruct (Meta, 2024) and Mistral-7B-Instruct-v0.2 (Jiang et al., 2023) as the backbone LLMs, both accessible via HuggingFace (Wolf et al., 2020). Our **ThinK** aims to prune channels of the KV, which is agnostic to KV cache compression methods. If there is no other statement, we prune the key cache by default. All the experiments are conducted using one Nvidia A100. To fairly compare KV cache compression methods and KV cache compression integrated with **ThinK**, we use the same hyperparameters for both. For example, when comparing SnapKV and SnapKV integrated with **ThinK**, we set the maximum pooling kernel size to 7 and the observation window size to 32, using the same KV-size for both.

4.2 Results on LongBench

Tables 2 and 3 present the results of KV compression methods and KV compression methods integrated with our channel pruning method of Key cache (**ThinK**) over two different base LLMs across various KV-sizes

Table 3: Performance comparison of Key cache pruning on Mistral-7B by ThinK on LongBench.

	Single	e-Docum	•		-Documen	•		mmariza			-shot Le	earning	Synt	hetic	С	ode	
Method	MrtvQA	Qasper	MF-en	HotpotQA	2WikiMQA	Musique	GovRepor	QMSum	MultiNews	TREC	TriviaQ.A	SAMSum	PCount	PRe	ν_{cc}	RB-P	Avg.
ALL KV	26.63	32.99	49.34	42.77	27.35	18.77	KV-si 32.87	ze Full 24.24	27.10	71.00	86.23	42.96	2.75	86.98	56.93	54.49	42.71
							KV-s	ize 128									
H2O	21.21	21.81	38.87	30.42	20.36	12.30	20.58	22.61	22.10	39.00	82.37	40.44	2.90	79.56	51.22	48.38	34.63
+ThinK(40) 21.17	21.90	39.29	29.92	20.99	12.30	20.84	22.91	21.92	39.00	82.70	40.35	2.97	79.21	51.19	48.32	34.69
+ThinK(50	21.67	21.80	39.48	28.74	20.65	13.14	20.57	22.83	21.78	39.00	82.54	40.12	3.61	78.39	50.27	48.4	34.56
+ThinK(60		21.30	39.56	28.68	21.29	13.97	20.13	22.52	21.81	39.50	82.05	39.14	4.16			47.67	
$\overline{\operatorname{Snap}}\overline{\operatorname{KV}}$	19.17	$2\overline{1.40}$	42.93	3 6 .7 6 _	$\bar{2}2.44$	15.86	19.16	21.84	21.55	-47.50	84.15	40.24	2.30	68.26	52.31	48.80	$\overline{35.29}$
+ThinK(40		21.00	42.65	37.58	22.09	15.23	19.29	22.01	21.22	47.00	83.85	39.64	3.20		51.48		35.16
+ThinK(50		20.60	43.37	37.27	21.58	15.66	19.06	21.79	21.02	47.00	83.38	39.77	3.65		50.80		35.06
+ ThinK (60) 21.25	20.82	44.20	36.21	21.68	16.47	19.05	21.99	20.73	45.00	83.81	38.79	4.19	66.90	49.99	47.61	34.92
							KV-s	ize 512									
H2O	21.83	26.00	44.69	32.46	23.05	14.69	23.53	23.06	24.59	42.00	85.22	41.49	3.40	86.20	54.78	51.09	37.38
+ThinK(40) 21.58	26.15	44.49	32.73	23.99	15.09	23.56	23.28	24.45	42.00	85.58	42.58	3.18	85.7	54.39	51.15	37.49
+ThinK(50) 22.76	25.74	44.61	31.74	23.25	13.91	23.31	23.13	24.34	41.00	85.39	41.85	2.82			50.88	
+ThinK(60		25.57	44.04	29.48	22.88	13.67	23.31	22.64	24.10	41.00	85.31	41.15	2.98			50.25	36.58
$\overline{\operatorname{Snap}}\overline{\operatorname{K}}\overline{\operatorname{V}}$	24.44	$^{-}2\overline{7}.8\overline{1}$	48.98	39.46	$\bar{2}5.\bar{2}5$	16.98	23.70	22.96	$\overline{24.37}$	$\overline{67.00}$	85.88	$-41.\overline{2}6^{-}$	2.78			53.41	40.46
+ThinK(40		28.46	49.26	38.13	24.22	16.92	23.59	23.70	24.46	67.50	85.9	42.51	2.92		55.89		40.40
+ThinK(50	,	29.22	48.59	37.70	24.27	17.39	23.68	23.65	24.58	67.50	86.05	42.01	3.07			53.29	
+ ThinK (60) 24.07	28.27	49.10	38.65	24.31	17.52	23.16	23.51	24.23	67.00	86.33	40.78	3.69	83.74	54.94	52.23	40.10
							KV-si	ze 1024									
H2O	23.67	28.55	46.40	36.99	24.82	15.02	25.21	23.04	25.77	46.00	85.93	41.98	3.24	86.57	56.40	52.75	38.90
+ThinK(40		28.91	45.84	35.78	24.88	14.55	25.11	23.35	25.83	45.50	86.11	42.44	3.23	84.82		53.02	38.72
+ThinK(50		28.40	46.60	35.57	24.26	14.78	24.98	23.31	25.68	44.50	86.16	42.72	3.38			52.63	
+ThinK(60		27.76	46.25	35.28	24.38	14.74	24.35	_ 23.35	25.50	44.50	85.38	41.37	3.34			51.89	
$\overline{\operatorname{Snap}}\overline{\operatorname{K}}\overline{\operatorname{V}}$	25.47	$^{-}2\overline{9}.57$	49.33	40.90 _	25.53	T9.01	25.94	- 2 3.89	26.21	$\overline{69.50}$	86.48	42.10	2.98				$\overline{41.64}$
+ThinK(40		30.48	48.58	41.11	25.28	18.99	25.91	24.00	26.13	70.00	86.64	43.35	2.98	86.3		54.19	$\frac{41.62}{11.62}$
+ThinK(50		30.08	49.41	40.59	25.13	19.58	25.47	24.23	25.92	69.5	86.67	42.31	2.74	84.78	57.43		41.44
+ ThinK (60) 24.69	29.3	48.90	40.44	25.33	19.58	25.23	23.6	25.25	69.00	86.85	40.86	3.19	83.70	56.3	53.30	40.97
								ze 2048									
H2O	25.76	31.10	49.06	40.38	26.43	16.78	27.17	23.64	26.69	55.00	86.35	42.48	2.72			53.91	
+ThinK(40		30.80	48.45	39.64	26.08	16.82	27.12	23.79	26.65	53.50	86.39	43.03	3.29			53.60	40.47
+ThinK(50		31.24	48.69	39.65	25.84	16.72	26.69	23.57	26.78	52.00	86.74	42.85	4.01			53.67	
+ThinK(60		31.00	48.23	38.58 _	_ 25.71_	_ 16.54	_ 26.51	_ 23.81	26.28	_50.50	86.57	42.05	3.36			52.67	
SnapKV	25.89	32.56	48.55	41.68	27.24	18.75	28.90	24.47	26.63	70.00	86.27	42.57	3.09			53.83	42.18
+ThinK(40		32.67	48.70	41.06	27.07	19.14	28.91	24.37	26.88	70.00	86.37	42.75	3.61			54.44	
+ThinK(50		32.94 32.53	49.02 48.73	40.86	26.84	19.49 18.92	28.46 27.40	24.51	26.72 26.37	70.00	86.50	41.75	$\frac{2.78}{3.31}$			54.15	
+ThinK(60	20.00	32.53	48.73	40.95	26.77	18.92	27.40	23.97	26.37	70.00	86.45	41.12	3.31	62.24	10.06	53.53	41.52

on LongBench. The following observations can be drawn: (1) Our method can further prune the channels of the key cache after compressing the KV cache with H2O and SnapKV. For the base model LLaMA3-8B, our method reduces memory usage and slightly improves performance for both H2O and SnapKV. For the base model Mistral-7B, our method reduces memory with only a slight drop in performance in some cases. (2) Comparing the results of SnapKV or H2O integrated with **ThinK** in Table 2 to SnapKV or H2O integrated with l_1 or l_2 norm shown in Table 1, our proposed query-based channel pruning shows better performance when the pruning ratio is 40% compared to no pruning. However, l_1 and l_2 norm methods cannot outperform the KV compression methods without pruning. (3) When the pruning ratio is small, performance tends to be better than when the pruning ratio is large. (4) When the KV-size is increased from 128 to 2048, the performance of our channel pruning method improves. Notably, with a KV cache size of 2048 and a pruning ratio of 40%, our method can even outperform the LLaMA3-8B with a full KV cache. The above observations indicate that our method is agnostic to existing KV cache compression methods and can further improve their performance and memory reduction. Additionally, query-based pruning is more effective than l_1 and l_2 norm for channel pruning in LLMs.

4.3 Results on Needle-in-a-Haystack

Table 4 presents the results of the Needle-in-a-Haystack test based on the SnapKV (Li et al., 2024) approach with KV cache size of input prompt from 128 to 2048. With a modest pruning ratio $\lambda = 40\%$, the accuracy of **ThinK** is consistently better or comparable than the original SnapKV across both LLaMA3 and Mistral with

different KV cache sizes. Such comparisons demonstrate that the proposed query-driven channel pruning can effectively retain the informative channels and discard the noisy ones. With a pruning ratio of $\lambda \geq 50\%$, we observe an accuracy drop with a small KV-cache size, particularly for 128 and 512 across both LLaMA3 and Mistral. However, **ThinK** is still able to obtain comparable performance with SnapKV when we have a larger KV cache size (i.e., 1024 and 2048). Intuitively, a larger pruning ratio with a smaller KV cache size could tend to lose more important information compared to a larger KV cache size. In addition, the performance on larger KV cache size also suggests **ThinK** is robust for long context retrieval tasks.

Figure 6 (a)-(d) visualize the Needle-in-a-Haystack test accuracy against different token lengths and depth percent. The KV cache size is configured to 128 and 1024, with pruning ratio λ equal to 40% and 50%, respectively. First, **ThinK** can maintain the original retrieval capability of SnapKV though the overall numerical accuracy is different (i.e., 77.8 vs 78.6 and 90.4 vs 90.6). Because **ThinK**achieves the same accuracy at most of the entries with different token limits and depths as Snap KV. In addition, **ThinK** also successfully retrieves some "needles" where SnapKV fails, leading to higher overall accuracy. The visualization results further demonstrate the robustness of **ThinK** in a fine-grained perspective and **ThinK** can enhance the original quantization approach.

Model	Method	λ	KV-size								
			128	512	1024	2048					
LLaMA3-8B	SnapKV	0	79.6	90.2	91.2	91.7					
	SnapKV+ ThinK	40	79.6	90.3	91.2	91.7					
	SnapKV+ ThinK	50	77.4	89.6	91.0	91.7					
Mistral-7B	SnapKV	0	77.8	89.5	90.4	90.8					
	SnapKV+ThinK	40	78.6	90.1	90.6	90.9					
	SnapKV+ThinK	50	78.1	90.1	90.8	91.1					
	SnapKV+ThinK	60	75.9	89.2	90.6	91.1					

Table 4: Needles-in-a-Haystack Test Results

4.4 Ablation Studies

Table 5: Performance comparison of pruning K cache using different recent-size.

	Single	-Docum	ent QA	Multi-Document QA			Summarization				Few-shot Learning			Synthetic		Code	
Recent-Size	MrtvQA	Qasper	MF-en	HotpotQA	2WikiMQA	Musique	GovReport	QMSum.	MultiNews	TREC	TriviaQA	SAMSum	PCount	PRe	rcc	RB-P	Avg.
						H2O	+ ThinK	$\lambda = 40\%$)								
0	24.40	27.50	45.42	35.17	24.45	13.02	27.65	23.88	26.86	53.50	86.06	41.73	3.01	83.42	55.12	51.32	38.91
32	25.40	30.80	48.45	39.64	26.08	16.82	27.12	23.79	26.65	53.50	86.39	43.03	3.29	86.39	56.61	53.60	40.47
128	25.69	30.93	48.32	39.63	26.08	16.82	27.18	23.92	26.62	53.50	86.39	42.96	3.29	86.39	56.77	53.60	40.51
						SnapKV	$V + \mathbf{Thinl}$	$K(\lambda = 40)$	%)								
0	24.94	28.58	45.78	39.59	25.40	15.92	29.50	24.05	26.72	70.00	85.60	41.38	2.97	84.00	55.27	52.39	40.76
32	25.77	32.67	48.70	41.06	27.07	19.14	28.91	24.37	26.88	70.00	86.37	42.75	3.61	87.38	57.21	54.44	42.27
128	25.75	32.49	48.61	41.01	27.18	19.14	28.79	24.64	26.77	70.00	86.37	42.77	3.61	87.13	57.19	54.39	42.24

Impact of Different Recent Sizes. Preserve the most recent KV embeddings (Zhang et al., 2024c; Li et al., 2024) is important for maintaining the performance of LLMs after KV cache compression. Note that a tradeoff exists: increasing the recent-size allows more infomation to be propagated, while increasing the cache size to be stored. To study its impacts, we evaluate the performance produced by three recent-size, namely 0, 32 and 128, on LongBench, using Mistral-7B-Instruct-v0.2 as the baseline model. The results are summarized in Table 5. One can observe that a recent-size of 32 yields superior performance than 0 in terms of averaged score on LongBench which demonstrates the importance of keeping the most recent KVs. On

Table 6: ablations with the same memory consumption.

		Single	-Docum	ent QA	Mult	i-Documen	t QA	Su	mmarizat	ion	Few	-shot Le	arning	Synt	hetic	С	ode	
Methods	Memory(M)	NrtvQA	Qasper	MF-en	HotpotQA	2WikiMQA	Musique	GovReport	QMSum	MultiNews	TREC	TriviaQ.A	SAMSum	PCount	PRe	Lcc	RB-P	Avg.
)	H2O										
Vanilla	54.5	21.29	20.69	37.66	28.65	21.08	14.01	20.20	22.11	21.33	38.50	82.55	39.87	3.66	78.14	50.32	48.54	34.29
ThinK	54.4	21.17	21.90	39.29	29.92	20.99	12.30	20.84	22.91	21.92	39.00	82.70	40.35	2.97	79.21	51.19	48.32	34.69
Vanilla	208.0	22.13	23.83	43.24	30.92	23.36	14.56	22.92	22.77	24.23	41.50	85.04	41.26	3.02	86.03	54.91	50.50	36.89
ThinK	208.0	21.58	26.15	44.49	32.73	23.99	15.09	23.56	23.28	24.45	42.00	85.58	42.58	3.18	85.7	54.39		
Vanilla	413.0	22.90	28.45	46.16	35.57	23.86	13.74	24.90	23.19	25.77	44.50	85.54	41.97	3.22	85.82		52.33	
ThinK	412.8	23.97	28.91	45.84	35.78	24.88	14.55	25.11	23.35	25.83	45.50	86.11	42.44	3.23	84.82		53.02	
Vanilla	822.5	25.51	30.23	48.23	39.72	25.56	16.75	26.98	23.81	26.47	50.50	86.43	42.09	2.78	85.57	57.4	53.42	
ThinK	822.4	25.40	30.80	48.45	39.64	26.08	16.82	27.12	23.79	26.65	53.50	86.39	43.03	3.29	86.39	56.61	53.60	40.47
							Sn	apKV										
Vanilla	54.5	19.25	19.95	42.80	35.88	21.96	14.59	18.76	21.71	20.70	46.00	84.12	39.43	2.59	65.36	51.39	47.81	34.52
ThinK	54.4	20.52	21.00	42.65	37.58	22.09	15.23	19.29	22.01	21.22	47.00	83.85	39.64	3.20	67.45	51.48	48.31	35.16
Vanilla	208.0	23.31	27.45	48.85	38.77	23.93	16.50	23.44	23.63	24.13	66.00	86.05	41.00	2.62	87.01	56.13	52.60	40.09
ThinK	208.0	24.27	28.46	49.26	38.13	24.22	16.92	23.59	23.70	24.46	67.50	85.90	42.51	2.92	85.32	55.89	53.35	40.40
Vanilla	413.0	24.24	29.53	49.13	40.48	25.05	18.74	25.46	23.64	25.60	68.00	86.14	41.42	3.03	88.55	57.08	53.86	41.25
ThinK	412.8	25.22	30.48	48.58	41.11	25.28	18.99	25.91	24.00	26.13	70.00	86.64	43.35	2.98	86.30	56.71	54.19	41.62
Vanilla	822.5	24.84	31.90	48.16	41.32	26.77	19.49	28.23	24.63	26.41	70.00	86.32	41.83	2.91	88.06		53.74	41.97
ThinK	822.4	25.77	32.67	48.7	41.06	27.07	19.14	28.91	24.37	26.88	70.00	86.37	42.75	3.61	87.38	57.21	54.44	42.27

the other hand, the performance of 32 and 128 is negligible, suggesting that maintaining the most recent 32 KVs suffices to preserve optimal performance.

tion. To ensure a fair comparison, we adjust the KV cache size of H2O or SnapKV to match the memory usage of H2O with ThinK or SnapKV with ThinK. For example, the KV cache size of H2O with ThinK is 128. Due to channel pruning of the key cache, the memory consumption of H2O with ThinK at a 128 KV-size is lower than H2O at a 128 KV-size. Therefore, the KV-size of H2O is adjusted from 128 to 109. Table 6 and Figure 5 present the results of these comparisons on LongBench. As the results show, H2O or SnapKV with ThinK deliver superior performance compared to H2O or SnapKV without ThinK while maintaining the same memory usage. This demonstrates that KV cache compression methods, com-

bined with our query-based channel pruning, can com-

press the KV cache more effectively and utilize memory

more efficiently.

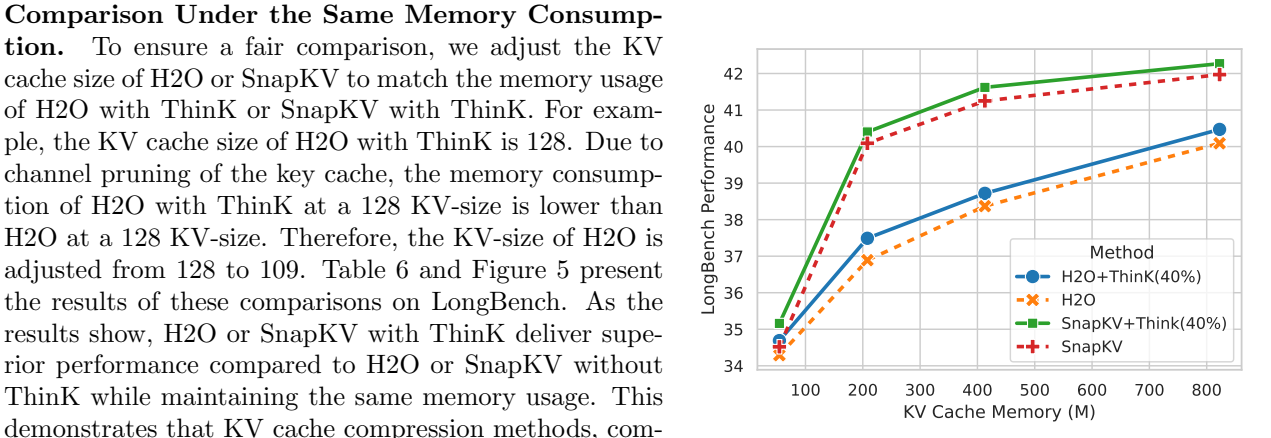


Figure 5: Performance comparisons under the same KV cache memory consumption.

Pruning Channels of Both Key and Value Cache. In our previous study, we evaluate methods with pruning channels of the key cache. In this part, we explore the impact of pruning channels of the value cache (Appendix A.1). Specifically, for KV cache compression methods, we prune channels of the key cache at one pruning ratio and channels of the value cache at another pruning ratio. Table 7 presents the results with LLaMA3-8B and Mistral-7B on LongBench. When testing on the base model LLaMA3-8B, H2O or SnapKV with key and value channel pruning can perform on par with H2O or SnapKV without channel pruning. In some cases, H2O or SnapKV with key and value channel pruning may even perform better. Pruning the channels of the value cache over the base model Mistral-7B experiences a slight performance drop. Despite this, note that KV cache with additional value channel pruning can further reduce memory usage.

Table 7: Performance comparison of pruning both K and V cache with different pruning ratios on LongBench. H2O + ThinK($\lambda_1 + \lambda_2$) indicates that H2O has $\lambda_1\%$ of the Key cache channels pruned and $\lambda_2\%$ of the Value cache channels pruned.

		Single	e-Docum	•		-Documen			mmariza			-shot Le	arning	Synthetic		Code		
	Method	NrtvQ.A	Qasper	MF-en	HotpotQA	2WikiMQl	Musique	GovRepor	QMSun	MultiNews	TREC	TriviaQA	SAMSum	PCount	PRe	Lec	RB-P	Avg.
	$\begin{array}{c} \text{H2O} \\ +\mathbf{ThinK}(30+30) \\ \hline \overline{\text{Snap}K}\overline{\mathbb{V}} \\ +\mathbf{ThinK}(30+30) \end{array}$	21.19	$ \begin{array}{r} 13.20 \\ -13.65 \\ 13.55 \\ 13.79 \end{array} $	$ \begin{array}{r} 31.61 \\ 33.08 \\ \hline 32.64 \\ 33.26 \end{array} $	37.79 - 41.86 - 38.75 40.93	$\begin{array}{r} 32.71 \\ -29.88 \\ \overline{29.64} \\ 29.39 \end{array}$	$- \frac{18.45}{18.04} - \frac{18.73}{19.22}$	KV-size 20.32 - 19.60 - 18.98 18.81	$\begin{array}{c} 128 \\ 22.02 \\ -21.65 \\ \hline 21.62 \\ 21.30 \end{array}$	$\begin{array}{r} 21.10 \\ -\frac{20.26}{20.26} \\ 19.26 \end{array}$	38.50 38.00 $4\overline{5.00}$ 41.50	87.75 86.08 88.36 87.00	$ \begin{array}{r} 39.14 \\ -38.61 \\ -\overline{37.64} \\ 37.95 \end{array} $	$\begin{array}{r} 5.83 \\ -5.16 \\ \hline 5.13 \\ 5.78 \end{array}$	$-\frac{69.50}{68.85}$	57.59 55.84	50.97 55.19 51.82 55.62	$\frac{35.74}{35.50}$ -
LLaMA3 8B	H2O + ThinK (30+30) SnapKV + ThinK (30+30)	24.84	17.93 17.57 23.96 24.59	$ \begin{array}{r} 34.68 \\ 34.18 \\ \hline 38.77 \\ 38.09 \end{array} $	$- \frac{42.11}{42.67} - \frac{42.75}{44.61}$	$ \begin{array}{r} 33.52 \\ -33.52 \\ -34.55 \\ 34.37 \end{array} $	$ \begin{array}{r} 19.92 \\ - \frac{19.95}{20.87} \\ 20.37 \end{array} $		$ \begin{array}{r} 512 \\ 22.56 \\ -22.23 \\ \hline 22.61 \\ 21.95 \end{array} $	$\begin{array}{r} 23.82 \\ -\frac{22.82}{23.97} \\ -23.30 \end{array}$	41.00 38.50 70.00 66.00	90.46 90.11 90.52 90.69	$ \begin{array}{r} 40.20 \\ 39.08 \\ -40.\overline{29} \\ 39.38 \end{array} $	5.87 -5.21 -5.81 5.60	$-\frac{69.0}{69.50}$	$\frac{59.99}{59.04}$	51.69 56.83 51.81 58.46	$\frac{37.23}{40.10}$ -
<u>.</u>	H2O + ThinK (30+30) + ThinK (40+40) SnapK∇ + ThinK (30+30) + ThinK (40+40)	$\frac{24.87}{25.86}$ 25.13	26.85 26.77 24.31 29.55 29.97 28.85	39.54 39.68 37.77 41.10 40.35 40.70	44.30 42.12 - 43.13 - 44.99 44.12 44.21	$ \begin{array}{r} 32.92 \\ 33.08 \\ 34.42 \\ \hline 35.80 \\ 34.64 \\ 36.36 \end{array} $	21.09 19.59 19.60 21.81 19.94 21.07	KV-size 24.68 23.00 - 21.67 - 25.98 23.62 22.31	2048 23.01 22.89 22.70 23.40 23.03 22.89	26.16 25.27 -24.52 -26.46 25.30 24.80	53.00 51.00 49.00 73.50 72.50 72.50	90.65 91.11 90.81 90.56 90.78 90.88	41.84 40.58 39.28 41.66 39.46 38.77	$\begin{array}{c} 4.91 \\ 5.23 \\ -6.00 \\ \hline 5.17 \\ 5.35 \\ 6.41 \end{array}$	$\begin{array}{r} 69.00 \\ -69.00 \\ \hline 69.25 \\ 69.00 \end{array}$	61.12 61.81 $\overline{58.67}$ 61.50	51.31 57.95 58.08 51.52 57.91 58.87	$ \begin{array}{r} 39.59 \\ 39.19 \\ \hline 41.58 \\ 41.41 \end{array} $
-	H2O + ThinK (30+30) SnapKV + ThinK (30+30)	19.17	$ \begin{array}{r} 21.81 \\ -21.49 \\ \hline 21.40 \\ 20.61 \end{array} $	$ \begin{array}{r} 38.87 \\ 38.01 \\ \hline 42.93 \\ 42.68 \end{array} $	30.42 - 30.66 - 36.76 37.63	$\begin{array}{r} 20.36 \\ -22.28 \\ \hline 22.\overline{44} \\ 23.19 \end{array}$	$ \begin{array}{r} 12.30 \\ -\frac{13.87}{15.86} \\ 15.09 \end{array} $	KV-size 20.58 - 20.13 - 19.16 18.97	$ \begin{array}{r} 128 \\ 22.61 \\ - 22.45 \\ \hline 21.84 \\ 21.93 \end{array} $	$\begin{array}{r} 22.10 \\ -21.07 \\ \overline{21.55} \\ 20.55 \end{array}$	39.00 38.50 47.50 45.00	82.37 82.20 84.15 84.06	$- 40.44 \\ - 38.69 \\ \overline{40.24} \\ 39.33$	$\begin{array}{r} 2.90 \\ -2.94 \\ 2.30 \\ 2.99 \end{array}$	$-\frac{78.56}{68.26}$	$\frac{51.55}{52.31}$	48.38 48.28 48.80 47.51	$\frac{34.46}{35.29}$ -
7B	H2O + ThinK (30+30) + ThinK (30+10) SnapKV + ThinK (30+30) + ThinK (30+10)	$\frac{22.14}{24.44}$ 24.10	26.00 24.26 25.15 -27.81 27.04 28.14	44.69 44.77 45.29 - 48.98 47.76 48.35	$ \begin{array}{r} 32.46 \\ 30.47 \\ -31.78 \\ \hline 39.46 \\ 38.66 \\ 39.03 \end{array} $	$23.05 \\ 22.94 \\ 23.21 \\ -25.25 \\ 25.45 \\ 24.83$	$ \begin{array}{r} 14.69 \\ 14.96 \\ -\frac{14.62}{16.98} \\ 17.51 \\ 16.68 \end{array} $		$\begin{array}{c} 512 \\ 23.06 \\ 22.90 \\ -22.70 \\ \hline 22.96 \\ 22.81 \\ 23.12 \end{array}$	24.59 23.73 -24.51 -24.37 -23.91 24.34	$\begin{array}{c} 42.00 \\ 41.50 \\ 41.50 \\ \hline 67.\overline{0} \\ 66.00 \\ 67.50 \end{array}$	85.22 85.30 85.61 85.88 86.62 86.09	$\begin{array}{r} 41.49 \\ 40.21 \\ -41.58 \\ \overline{41.26} \\ 39.91 \\ 41.69 \end{array}$	$ \begin{array}{r} 3.40 \\ 3.08 \\ -2.75 \\ 2.78 \\ 3.36 \\ 2.65 \end{array} $	$\begin{array}{r} 80.07 \\ -84.03 \\ -86.56 \\ 82.24 \end{array}$	54.48 54.50 $\overline{56.46}$ 55.96	51.09 50.96 51.09 53.41 52.81 53.22	$ \begin{array}{r} 36.54 \\ \hline 37.11 \\ \hline 40.46 \\ 39.80 \end{array} $
Mistral	H2O + ThinK (30+30) + ThinK (30+10) SnapkV + ThinK (30+30) + ThinK (30+10)	$\frac{24.13}{25.47}$ 25.29	28.55 26.54 28.57 29.57 29.25 29.30	46.4 47.00 -46.31 -49.33 49.17 49.56	36.99 35.52 - 35.59 - 40.90 41.25 41.44	$ \begin{array}{r} 24.82 \\ 24.79 \\ 24.92 \\ -25.53 \\ 25.75 \\ 25.29 \end{array} $	$ \begin{array}{r} 15.02 \\ 17.15 \\ -\frac{15.34}{19.01} \\ 19.37 \\ 19.02 \end{array} $	KV-size 25.21 23.64 - 24.58 - 25.94 24.64 25.21	$ \begin{array}{r} 1024 \\ 23.04 \\ 23.12 \\ -\frac{23.33}{23.89} \\ 23.02 \\ 23.73 \end{array} $	25.77 25.20 -25.93 -26.21 25.27 25.72	46.00 44.00 45.50 69.50 69.00 69.00	85.93 86.38 85.91 86.48 86.70 86.69	$ 41.98 41.67 -42.97 -42.\overline{10} 40.92 42.55 $	3.24 3.46 2.57 2.98 3.29 2.44	$\begin{array}{r} 80.14 \\ -83.64 \\ -88.56 \\ 82.06 \end{array}$	55.39 57.19 57.15	52.86 52.73	$ \begin{array}{r} 38.23 \\ 38.59 \\ \hline 41.64 \\ 41.02 \end{array} $
-	H2O +ThinK(30+30) +ThinK(30+10) SnapkV +ThinK(30+30) +ThinK(30+10)	$\begin{array}{r} 25.64 \\ \hline 25.89 \\ 27.01 \end{array}$	31.10 28.74 30.65 32.56 30.72 32.69	49.06 47.54 48.95 48.55 48.81 48.96	40.38 38.67 - 40.42 - 41.68 41.15 40.83	$ \begin{array}{r} 26.43 \\ 26.25 \\ 26.43 \\ \hline 27.24 \\ 26.93 \\ 26.70 \end{array} $	$ \begin{array}{r} 16.78 \\ 17.35 \\ -\frac{16.65}{18.75} \\ 18.93 \\ 19.02 \end{array} $		2048 23.64 23.27 - 23.51 - 24.47 23.59 24.23	26.69 26.15 -26.59 -26.63 -26.42 26.64	55.0 51.00 52.50 70.00 70.00 70.00	86.35 87.01 86.53 86.27 86.82 86.65	42.48 43.02 $-\frac{43.45}{42.57}$ 41.91 42.63	2.72 2.94 2.66 3.09 3.05 2.22	81.46 83.96 86.93 82.65	57.44 57.01		$ \begin{array}{r} 39.64 \\ \underline{40.32} \\ \hline 42.18 \\ 41.57 \end{array} $

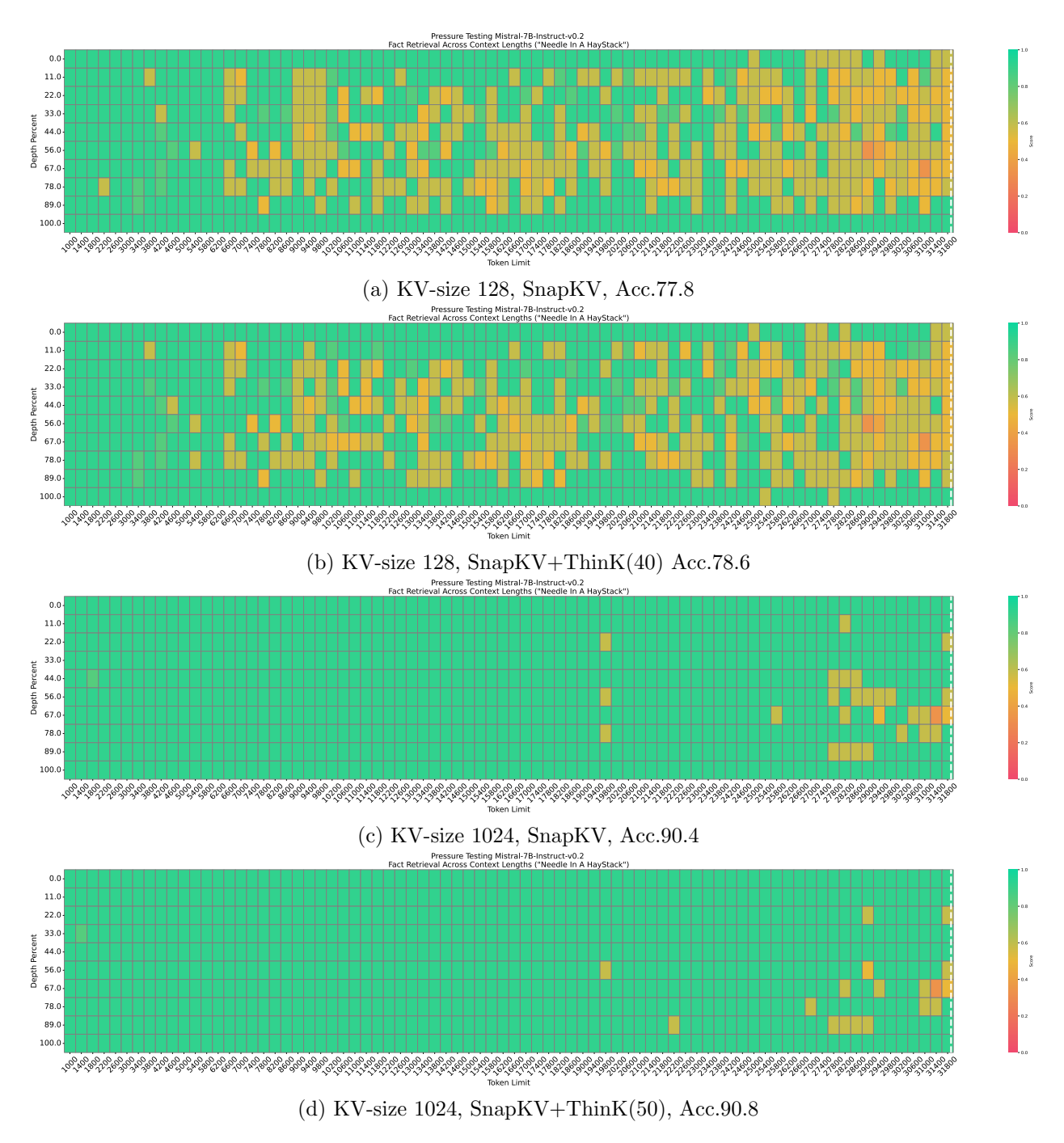


Figure 6: Needle-in-a-Haystack test performance comparison with Mistral-7B-Instruct-v0.2.

5 Related Work

In scenarios involving long contexts, the most significant computational burden from the attention mechanism is the key-value (KV) cache. Reducing the KV cache is a high priority for optimizing deployment efficiency. System-level optimizations, such as FlashAttention (Dao, 2023) and PagedAttention (Kwon et al., 2023), have been developed to address this issue. Additionally, algorithm-level optimizations are being explored to further enhance efficiency.

KV Cache Eviction. StreamingLLM (Xiao et al., 2023b) maintains a few initial tokens and some recent tokens based on the observation of attention sink, which may result in the loss of important information carried by the dropped tokens. H2O (Zhang et al., 2024c) retains only a small portion of the tokens by greedily dropping tokens based on their contributions to the cumulative attention. SnapKV (Li et al., 2024) selects clustered important KV positions for each attention head from an 'observation' window located at the end of the prompts. FastGen (Ge et al., 2023) adaptively evicts tokens from attention heads that emphasize local contexts. This approach focuses on discarding non-special tokens centered on special tokens, while the standard KV cache is used only for attention heads that broadly attend to all tokens. PyramidKV (Zhang et al., 2024b) and PyramidInfer (Yang et al., 2024) considers adjusting the KV cache size across different layers by allocating more cache in the lower layers and less in the higher ones.

KV Cache Quantization. SmoothQuant (Xiao et al., 2023a) can quantize the KV cache to 8-bit with minimal performance degradation. Q-Hitter (Zhang et al., 2024c) uses accumulated attention scores and 'Quantization Friendliness' metrics to identify tokens that are essential for maintaining the generalization capabilities of LLMs and are suitable for KV cache quantization. Some studies have found that the key cache and value cache should be quantized differently (Liu et al., 2024b; Hooper et al., 2024): the key cache should be quantized per-channel, while the value cache should be quantized per-token.

Structured Pruning of LLMs. Structured pruning (Ma et al., 2023; Ding et al., 2023) of LLMs traditionally focuses on removing unimportant layers, heads, and hidden dimensions, which often results in significant performance degradation. In contrast, our methodology preserves the original architecture of the LLM and specifically targets the channel dimension within each head's key cache. By dynamically identifying unimportant channels based on data dependant criterion, our approach greatly reduce the key cache-size with negligible performance loss.

6 End Note and Future Direction

Motivated by the observation that certain channels have significantly larger magnitudes compared to others, and the singular value analysis indicates that the key cache is inherently low-rank (Singhania et al., 2024), we propose **ThinK** to perform pruning over the key cache channel. The proposed pruning strategy is query-dependant and optimized based on the attention scores, ensuring that essential information is retained for each input query. In addition, **ThinK** can be seamlessly integrated with other popular token-level KV cache quantization techniques (Li et al., 2024; Zhang et al., 2024c), further enhancing inference efficiency. Extensive experiments on LongBench (Bai et al., 2023) and Needle-in-a-Haystack tests with two foundation models demonstrate the effectiveness and robustness of our query-dependent channel pruning method. Our approach achieves comparable or superior performance to baseline methods while reducing the key cache size by 40%. Our analysis indicates that **ThinK** can maintain superior performance over baselines with a smaller KV cache size under equivalent memory consumption conditions.

Future work will focus on strategies to increase the pruning ratio without compromising model performance, and exploring pruning techniques for value caches. We also plan to evaluate channel importance from a more sophisticated and compositional perspective, incorporating both token-level and channel-level information

References

- Ainslie, J., Lee-Thorp, J., de Jong, M., Zemlyanskiy, Y., Lebrón, F., and Sanghai, S. (2023). Gqa: Training generalized multi-query transformer models from multi-head checkpoints. arXiv preprint arXiv:2305.13245.
- Bai, Y., Lv, X., Zhang, J., Lyu, H., Tang, J., Huang, Z., Du, Z., Liu, X., Zeng, A., Hou, L., et al. (2023). Longbench: A bilingual, multitask benchmark for long context understanding. arXiv preprint arXiv:2308.14508.
- Bhojanapalli, S., Chakrabarti, A., Jain, H., Kumar, S., Lukasik, M., and Veit, A. (2021). Eigen analysis of self-attention and its reconstruction from partial computation. arXiv preprint arXiv:2106.08823.
- Blalock, D., Gonzalez Ortiz, J. J., Frankle, J., and Guttag, J. (2020). What is the state of neural network pruning? *Proceedings of machine learning and systems*, 2:129–146.
- Bordes, A., Boureau, Y.-L., and Weston, J. (2016). Learning end-to-end goal-oriented dialog. arXiv preprint arXiv:1605.07683.
- Brandon, W., Mishra, M., Nrusimha, A., Panda, R., and Kelly, J. R. (2024). Reducing transformer key-value cache size with cross-layer attention. arXiv preprint arXiv:2405.12981.
- Brown, T., Mann, B., Ryder, N., Subbiah, M., Kaplan, J. D., Dhariwal, P., Neelakantan, A., Shyam, P., Sastry, G., Askell, A., et al. (2020). Language models are few-shot learners. Advances in neural information processing systems, 33:1877–1901.
- Chen, B., Dao, T., Winsor, E., Song, Z., Rudra, A., and Ré, C. (2021a). Scatterbrain: Unifying sparse and low-rank attention. Advances in Neural Information Processing Systems, 34:17413–17426.
- Chen, M., Tworek, J., Jun, H., Yuan, Q., Pinto, H. P. D. O., Kaplan, J., Edwards, H., Burda, Y., Joseph, N., Brockman, G., et al. (2021b). Evaluating large language models trained on code. arXiv preprint arXiv:2107.03374.
- Dao, T. (2023). Flashattention-2: Faster attention with better parallelism and work partitioning. arXiv preprint arXiv:2307.08691.
- Demmel, J. W. (1997). Applied numerical linear algebra. SIAM.
- Dettmers, T., Pagnoni, A., Holtzman, A., and Zettlemoyer, L. (2024). Qlora: Efficient finetuning of quantized llms. Advances in Neural Information Processing Systems, 36.
- Ding, N., Chen, Y., Xu, B., Qin, Y., Zheng, Z., Hu, S., Liu, Z., Sun, M., and Zhou, B. (2023). Enhancing chat language models by scaling high-quality instructional conversations. arXiv preprint arXiv:2305.14233.
- Dong, H., Xiong, W., Pang, B., Wang, H., Zhao, H., Zhou, Y., Jiang, N., Sahoo, D., Xiong, C., and Zhang, T. (2024a). Rlhf workflow: From reward modeling to online rlhf. arXiv preprint arXiv:2405.07863.
- Dong, H., Yang, X., Zhang, Z., Wang, Z., Chi, Y., and Chen, B. (2024b). Get more with less: Synthesizing recurrence with kv cache compression for efficient llm inference. arXiv preprint arXiv:2402.09398.
- Frankle, J. and Carbin, M. (2018). The lottery ticket hypothesis: Finding sparse, trainable neural networks. arXiv preprint arXiv:1803.03635.

- Frantar, E., Ashkboos, S., Hoefler, T., and Alistarh, D. (2022). Gptq: Accurate post-training quantization for generative pre-trained transformers. arXiv preprint arXiv:2210.17323.
- Ge, S., Zhang, Y., Liu, L., Zhang, M., Han, J., and Gao, J. (2023). Model tells you what to discard: Adaptive kv cache compression for llms. arXiv preprint arXiv:2310.01801.
- Hadi, M. U., Qureshi, R., Shah, A., Irfan, M., Zafar, A., Shaikh, M. B., Akhtar, N., Wu, J., Mirjalili, S., et al. (2023). Large language models: A comprehensive survey of its applications, challenges, limitations, and future prospects. *TechRxiv*.
- Hoffmann, J., Borgeaud, S., Mensch, A., Buchatskaya, E., Cai, T., Rutherford, E., Casas, D. d. L., Hendricks, L. A., Welbl, J., Clark, A., et al. (2022). Training compute-optimal large language models. arXiv preprint arXiv:2203.15556.
- Hooper, C., Kim, S., Mohammadzadeh, H., Mahoney, M. W., Shao, Y. S., Keutzer, K., and Gholami, A. (2024). Kvquant: Towards 10 million context length llm inference with kv cache quantization. arXiv preprint arXiv:2401.18079.
- Hu, E. J., Shen, Y., Wallis, P., Allen-Zhu, Z., Li, Y., Wang, S., Wang, L., and Chen, W. (2021). Lora: Low-rank adaptation of large language models. arXiv preprint arXiv:2106.09685.
- Jia, Z., Maggioni, M., Staiger, B., and Scarpazza, D. P. (2018). Dissecting the nvidia volta gpu architecture via microbenchmarking. arXiv preprint arXiv:1804.06826.
- Jiang, A. Q., Sablayrolles, A., Mensch, A., Bamford, C., Chaplot, D. S., Casas, D. d. l., Bressand, F., Lengyel, G., Lample, G., Saulnier, L., et al. (2023). Mistral 7b. arXiv preprint arXiv:2310.06825.
- Kamradt, G. (2023). Needle In A Haystack pressure testing LLMs. Github.
- Kaplan, J., McCandlish, S., Henighan, T., Brown, T. B., Chess, B., Child, R., Gray, S., Radford, A., Wu, J., and Amodei, D. (2020). Scaling laws for neural language models. arXiv preprint arXiv:2001.08361.
- Kwon, W., Li, Z., Zhuang, S., Sheng, Y., Zheng, L., Yu, C. H., Gonzalez, J., Zhang, H., and Stoica, I. (2023). Efficient memory management for large language model serving with pagedattention. In *Proceedings of the 29th Symposium on Operating Systems Principles*, pages 611–626.
- Leviathan, Y., Kalman, M., and Matias, Y. (2023). Fast inference from transformers via speculative decoding. In *International Conference on Machine Learning*, pages 19274–19286. PMLR.
- Li, Y., Huang, Y., Yang, B., Venkitesh, B., Locatelli, A., Ye, H., Cai, T., Lewis, P., and Chen, D. (2024). Snapkv: Llm knows what you are looking for before generation. arXiv preprint arXiv:2404.14469.
- Lin, J., Tang, J., Tang, H., Yang, S., Chen, W.-M., Wang, W.-C., Xiao, G., Dang, X., Gan, C., and Han, S. (2024). Awq: Activation-aware weight quantization for on-device llm compression and acceleration. Proceedings of Machine Learning and Systems, 6:87–100.
- Liu, A., Liu, J., Pan, Z., He, Y., Haffari, G., and Zhuang, B. (2024a). Minicache: Kv cache compression in depth dimension for large language models. arXiv preprint arXiv:2405.14366.
- Liu, Z., Yuan, J., Jin, H., Zhong, S., Xu, Z., Braverman, V., Chen, B., and Hu, X. (2024b). Kivi: A tuning-free asymmetric 2bit quantization for kv cache. arXiv preprint arXiv:2402.02750.
- Ma, X., Fang, G., and Wang, X. (2023). Llm-pruner: On the structural pruning of large language models. Advances in neural information processing systems, 36:21702–21720.
- Meta, A. (2024). Introducing meta llama 3: The most capable openly available llm to date. Meta AI.
- OpenAI (2022). OpenAI: Introducing ChatGPT.

- OpenAI (2023). Gpt-4 technical report. arXiv preprint arXiv:2303.08774.
- Reid, M., Savinov, N., Teplyashin, D., Lepikhin, D., Lillicrap, T., Alayrac, J.-b., Soricut, R., Lazaridou, A., Firat, O., Schrittwieser, J., et al. (2024). Gemini 1.5: Unlocking multimodal understanding across millions of tokens of context. arXiv preprint arXiv:2403.05530.
- Scao, T. L., Fan, A., Akiki, C., Pavlick, E., Ilić, S., Hesslow, D., Castagné, R., Luccioni, A. S., Yvon, F., Gallé, M., et al. (2022). Bloom: A 176b-parameter open-access multilingual language model. arXiv preprint arXiv:2211.05100.
- Singhania, P., Singh, S., He, S., Feizi, S., and Bhatele, A. (2024). Loki: Low-rank keys for efficient sparse attention. arXiv preprint arXiv:2406.02542.
- Strubell, E., Ganesh, A., and McCallum, A. (2020). Energy and policy considerations for modern deep learning research. In *Proceedings of the AAAI conference on artificial intelligence*, volume 34, pages 13693–13696.
- Touvron, H., Lavril, T., Izacard, G., Martinet, X., Lachaux, M.-A., Lacroix, T., Rozière, B., Goyal, N., Hambro, E., Azhar, F., et al. (2023a). Llama: Open and efficient foundation language models. arXiv preprint arXiv:2302.13971.
- Touvron, H., Martin, L., Stone, K., Albert, P., Almahairi, A., Babaei, Y., Bashlykov, N., Batra, S., Bhargava, P., Bhosale, S., et al. (2023b). Llama 2: Open foundation and fine-tuned chat models. arXiv preprint arXiv:2307.09288.
- Vaswani, A., Shazeer, N., Parmar, N., Uszkoreit, J., Jones, L., Gomez, A. N., Kaiser, Ł., and Polosukhin, I. (2017). Attention is all you need. *Advances in neural information processing systems*, 30.
- Wan, Z., Wang, X., Liu, C., Alam, S., Zheng, Y., Qu, Z., Yan, S., Zhu, Y., Zhang, Q., Chowdhury, M., et al. (2023). Efficient large language models: A survey. arXiv preprint arXiv:2312.03863, 1.
- Wang, S., Li, B. Z., Khabsa, M., Fang, H., and Ma, H. (2020). Linformer: Self-attention with linear complexity. arXiv preprint arXiv:2006.04768.
- Wolf, T., Debut, L., Sanh, V., Chaumond, J., Delangue, C., Moi, A., Cistac, P., Rault, T., Louf, R., Funtowicz, M., et al. (2020). Transformers: State-of-the-art natural language processing. In *Proceedings of the 2020 conference on empirical methods in natural language processing: system demonstrations*, pages 38–45.
- Wu, H. and Tu, K. (2024). Layer-condensed kv cache for efficient inference of large language models. arXiv preprint arXiv:2405.10637.
- Xiao, G., Lin, J., Seznec, M., Wu, H., Demouth, J., and Han, S. (2023a). Smoothquant: Accurate and efficient post-training quantization for large language models. In *International Conference on Machine Learning*, pages 38087–38099. PMLR.
- Xiao, G., Tian, Y., Chen, B., Han, S., and Lewis, M. (2023b). Efficient streaming language models with attention sinks. arXiv preprint arXiv:2309.17453.
- Xiong, W., Liu, J., Molybog, I., Zhang, H., Bhargava, P., Hou, R., Martin, L., Rungta, R., Sankararaman, K. A., Oguz, B., et al. (2023). Effective long-context scaling of foundation models. arXiv preprint arXiv:2309.16039.
- Xu, Y., Xie, L., Gu, X., Chen, X., Chang, H., Zhang, H., Chen, Z., Zhang, X., and Tian, Q. (2023). Qa-lora: Quantization-aware low-rank adaptation of large language models. arXiv preprint arXiv:2309.14717.
- Yang, D., Han, X., Gao, Y., Hu, Y., Zhang, S., and Zhao, H. (2024). Pyramidinfer: Pyramid kv cache compression for high-throughput llm inference. arXiv preprint arXiv:2405.12532.

- Zhang, T., Ladhak, F., Durmus, E., Liang, P., McKeown, K., and Hashimoto, T. B. (2024a). Benchmarking large language models for news summarization. *Transactions of the Association for Computational Linquistics*, 12:39–57.
- Zhang, X., Wei, F., and Zhou, M. (2019). Hibert: Document level pre-training of hierarchical bidirectional transformers for document summarization. arXiv preprint arXiv:1905.06566.
- Zhang, Y., Gao, B., Liu, T., Lu, K., Xiong, W., Dong, Y., Chang, B., Hu, J., Xiao, W., et al. (2024b). Pyramidkv: Dynamic kv cache compression based on pyramidal information funneling. arXiv preprint arXiv:2406.02069.
- Zhang, Z., Sheng, Y., Zhou, T., Chen, T., Zheng, L., Cai, R., Song, Z., Tian, Y., Ré, C., Barrett, C., et al. (2024c). H2o: Heavy-hitter oracle for efficient generative inference of large language models. *Advances in Neural Information Processing Systems*, 36.

A Additional Experimental Details

A.1 Value Cache Pruning

Similar to the approach used for the Key cache, the pruning of channels in the Value cache can be guided by two primary criteria: magnitude-based pruning and query-driven pruning. We find that query-driven pruning is still better than magnitude based pruning.

$$Score_{v,i}(\mathbf{Q}_i, \mathbf{K}_i, \mathbf{V}_i)[j] = \|softmax(\frac{\mathbf{Q}_i[-S_{obs}:]\mathbf{K}_i^T}{\sqrt{D}})\mathbf{V}_i[:,j]\|_F$$
(10)

$$I_i = \mathbf{Top}_T(\mathbf{Score}_{v,i}, T) \tag{11}$$

where $\mathbf{Q}_i, \mathbf{K}_i, \mathbf{V}_i \in \mathbb{R}^{S \times D}$. We define a criterion $\mathrm{Score}_{v,i}$ to indicate the importance of each channel in the head i of value cache. Then, only top T channels are retained.